Low-temperature electron-phonon heat transfer in metal films

S. Cojocaru and D. V. Anghel
Horia Hulubei National Institute for Physics and Nuclear Engineering, RO-077125 Magurele, Romania
(Received 16 August 2015; published 7 March 2016)

We consider the deformation potential mechanism of the electron-phonon coupling in metal films and investigate the intensity of the associated heat transfer between the electron and phonon subsystems. The focus is on the temperature region below dimensional crossover $T < T^*$ where the thermally relevant vibrations are described in terms of a quasi-two-dimensional elastic medium, while electron excitations behave as a three-dimensional Fermi gas. We derive an explicit expression for the power $P(T)$ of the electron-phonon heat transfer which explains the behavior observed in some experiments including the case of metallic film supported by an insulating membrane with different acoustic properties. It is shown that at low temperatures the main contribution is due to the coupling with Lamb's dilatational and flexural acoustic modes.

DOI: 10.1103/PhysRevB.93.115405

I. INTRODUCTION

In modern electronic devices the nanoscale miniaturization and sub-Kelvin temperatures are quite common, however the physical phenomena taking place in such conditions are far from complete understanding and attract a great deal of research interest. In this work we address an aspect of the electron-phonon interaction in confined systems related to heat transfer between electrons and phonons. This is an open problem in the fundamental sense with a direct connection to current research activity and important applications in a variety of fields from nanoelectronics to astrophysics. For instance, in a recent paper [1] the principle of electronic cooling [2] has been used to realize the "coolest microfridge" reaching a record temperature of less than 30 mK. In a typical setup a cooled metal part is suspended or mounted on an insulating support layer in contact with superconductors forming two symmetrically biased NIS (normal metal-insulator-superconductor) tunnel junctions. In this setup "hot" electrons from above the Fermi level are evacuated from the normal metal island, while "cold" electrons are injected below the Fermi level. Such microdevices can be mounted directly on a chip for cooling qubits or ultrasensitive low-temperature detectors, e.g., bolometers or calorimeters, where the biased NIS tunnel junctions can also be used for precision thermometry down to milli-Kelvin temperatures [3]. An important physical phenomenon controlling the cooling power is the heat transfer between electrons and phonons mediated by their coupling, $H_{e\text{-}p}$, when phonons are emitted and absorbed by electrons. When electrons are heated by an external source in a stationary regime one can assume their energy distribution to be characterized by a temperature T_e while the distribution of phonons corresponds to some lower temperature T_p. In many situations the temperature gradients are sufficiently small so that we also assume that space variation of T_e and T_p can be neglected. When both subsystems are bulklike (three-dimensional) the rate P at which electron energy is transferred to phonons has been obtained by considering the deformation-potential mechanism of electron-phonon coupling, which relates the local density fluctuation to the variation of the Fermi energy [4], and $P(T)$ has been shown to vary as T^5 at low temperatures (see, e.g., [5–7]):

$$P = \Sigma V_{el}\left(T_e^5 - T_p^5\right). \tag{1}$$

Here V_{el} is the volume of the metal and Σ depends on the electron-phonon coupling and other properties of the sample. This form has been derived for simple metals in the case when disorder is not strong ($ql \gg 1$, where q is the phonon wave vector and l is the electron mean free path) and which is also assumed in the present work. It should be mentioned that for disordered films a form with a stronger (T^6) low-temperature behavior has been found [8,9]. The dependence in Eq. (1) was confirmed in many experimental situations and is a standard formula assumed for the analysis of experimental data, e.g., [1,3]. However, the finite thickness of a film L eliminates the possibility of longer waves to propagate in this direction. Consequently, when temperatures fall below the dimensional crossover threshold $T < T^* \simeq c\hbar/(k_B L)$, where c is the sound velocity, the wavelength of the thermally relevant phonons becomes longer than L and we may treat the phonon subsystem in terms of a confined elastic medium. Respectively, thermal properties, including the electron-phonon heat transfer, are dominated by the vibrational eigenmodes corresponding to such a quasi-two-dimensional geometry. For values of L of the order of 100 nm and for sound velocities of the order of 10 km/s, the value of T^* is of the order of 1 K. Therefore size related effects in electron-phonon systems have become an important part of the physics at the nanoscale, e.g., [10,11]. In a number of experimental studies it has been found that the temperature dependence is best represented by the T^x with significantly lower values of x [12–14]. On the other hand, a theoretical investigation of the surface effects for a half-space geometry [15], including the surface specific Rayleigh phonon modes, has shown that the value of x is actually larger than 5 and at sufficiently low temperatures it exceeds 6. It should be mentioned that, since the Rayleigh waves are localized within a distance of the order of the wavelength from the surface, this description is valid for sufficiently thick layers, $qL \gg 1$. Thus, the growth of the exponential x with decreasing temperature has been later qualitatively confirmed in some experiments when metallic films were deposited on bulky substrates [13,16]. For a quasi-one-dimensional geometry (metallic nanowire) the model has been studied theoretically in [17] where the T^3 analog of Eq. (1) has been obtained. Although in [18] it was argued that for Al nanowires with 65×90-nm cross-section a better fit is achieved with the standard exponential $x = 5$, the results are still inconclusive

 ©2016 American Physical Society

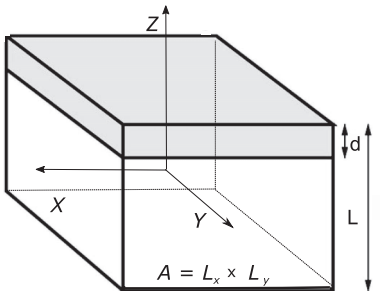

FIG. 1. Insulating membrane of thickness $L - d$ covered with a metal film (gray) of thickness d and surface area A.

since no dimensional crossover was observed around the anticipated temperature, 0.45 K. In contrast, a clear indication of a quasi-two-dimensional crossover in electron-phonon dominated heat flow with a distinct power law ($x < 4.5$) has been reported in [12,13]. Remarkably, the respective samples had also a strongly enhanced density of the heat flux compared to the thicker samples, which remained in the "bulk" regime and did not show a crossover behavior for the considered temperature interval. Typically, the metallic film is either deposited on an insulating membrane, Fig. 1, or suspended on top of superconducting electrodes [1].

The phonon spectrum of a quasi-two-dimensional system is quite different from that of a bulk. Vibrational eigenstates of such a slablike structure cannot be separated into longitudinal and transverse waves; instead in the elastic continuum approximation the spectrum is given by the Lamb eigenmodes (in addition to shear waves) actually representing a mixture of both [19]. The electron scattering by Lamb phonon modes has been studied earlier for semiconductor quantum wells (QWs) in [10,20] and in a double heterostructure QW including the piezoelectric coupling in [21]. It has been shown that the scattering rate τ^{-1} is dominated by coupling to the flexural acoustic mode (e.g., $\tau^{-1} \sim T^{5/2}, T^{7/2}$) due to its characteristic quadratic dispersion and high density of states, in contrast to the "standard" linear dispersion of the, e.g., dilatational Lamb mode, which has a negligible contribution (e.g., $\tau^{-1} \sim T^6$). In the present work the electron excitations in the metal film are treated as a three-dimensional Fermi gas interacting with the quasi-two-dimensional phonon subsystem. Thus, electrons are described by the parabolic dispersion with an effective electron mass $\epsilon_{\mathbf{k}} = \hbar^2\mathbf{k}^2/2m$ [notations for the components of the wave vector $\mathbf{k} = (\mathbf{k}_\parallel, k_z)$ correspond to Fig. 1] and a plane-wave function $\Psi_{\mathbf{k}}(\mathbf{r},\mathbf{t}) = \exp(i\mathbf{kr} - i\epsilon t/\hbar)/\sqrt{V_e} = \psi(k_z;z)\exp(i\mathbf{k}_\parallel\mathbf{r}_\parallel - i\epsilon t/\hbar)/\sqrt{A}$, where the electronic volume is $V_e = dA$ and $\psi(k_z;z)$ is given in the next section. We will use alternatively either the cylindrical coordinate system with k_z normal to the film and the in-plane vector $\mathbf{k}_\parallel$ at angle ϕ or the spherical system with the two angles denoted as θ and φ and $k = |\mathbf{k}|$. It should be mentioned that in ultrathin metal films electron confinement can result in the formation of the quantum-well state with $\psi(k_z;z) \sim \sin(k_z z)$ and $k_z = n\pi/d$, where the quantum numbers $n = 1,2,3,\ldots$ correspond to the electron quasi-two-dimensional energy sub-bands. However, in contrast to semiconductors, the QW state is more difficult to observe in metal films thicker than a few nm (see, e.g., [22]), because the electron de Broglie wavelength is comparable to the interatomic distance and signatures of size quantization are easily smeared out by film imperfections of the same length scale, e.g., surface roughness. Thus, the plane-wave form of $\psi(k_z;z)$ is an approximation, which is meant to describe the situation of a not very thin film where electron band structure can still be viewed as bulklike, while the phonon spectrum is dominated by quasi-two-dimensional modes. An important distinctive feature of this situation is that, although the phonons propagate parallel to the plane of the film, they can nevertheless produce electron scattering with a change of momentum in the direction normal to the plane, i.e., $\hbar k_z' \neq \hbar k_z$. This paradox is due to the displacement field pattern characteristic of the Lamb waves (see below) which allows electrons to couple both to longitudinal (in-plane) and transverse (out-of -plane) components of the vibrations (see also the discussion in [23] for the case of a nanowire). The effect pertains primarily to the flexural modes and leads to a nontrivial modification of the heat transfer.

In an often used experimental setup the metallic strip is in contact with an insulating support membrane which can modify both the phonon spectrum and the flow of the heat produced in the metal and transmitted through the boundaries (e.g., [24]). Thus, the boundary can give rise to interface guided Stoneley phonon modes [25,26]. However, for a solid-solid boundary the conditions on the parameters of the media (densities and sound velocities) required for the existence of Stoneley modes are very restrictive (see, e.g., [27]). We return to this issue in the next chapter. The heat transfer can also depend on the coupling of phonons in the film to their own bath; e.g., in [16,28] it has been found that the distribution of phonons available for interaction with electrons in metal films can remain relatively unaffected by the substrate. In general, due to a mismatch of properties on the interface between two materials the phonons will scatter and produce a thermal boundary resistance; the associated Kapitza heat flow then depends on the difference of phonon temperatures of the two materials and is usually given by $\kappa(T_{p,1}^4 - T_{p,2}^4)$ [29,30]. There are other effects that can contribute to the heat transport, e.g., related to the operational principle of electron microcoolers, when there exists a heat backflow from the superconductor to the metal island [31].

Below we will consider the heat flux derived from the electron-phonon coupling for the structure shown in Fig. 1 by first assuming homogeneous elastic properties of the compound slab of volume $V_p = L \times A$ [21], its total mass M, and mass density $\rho = M/V_p$. The case of a suspended metallic film corresponds to the condition $L = d$. To account for the modification of the phonon spectrum when the metal film is deposited on the insulating membrane with acoustic characteristics different from the metal, one can consider different models of their bonding (see, e.g., [32]), however we assume that the contact between the two media is rigid. It should be stressed that knowledge of the phonon spectrum is not sufficient when considering the coupling to electrons and one should also determine the properly normalized amplitudes of the phonon field.

II. ELECTRON-PHONON COUPLING AT LOW TEMPERATURES

We define the rectangular coordinate system in such a way that $z = \pm L/2$ corresponds to the top and bottom surfaces of

the slab. Elastic vibrations are described by the vector field of relative displacements $\mathbf{u} = \mathbf{u}(\mathbf{r})$ [19] expanded in the series of quantized eigenmodes of the continuum elasticity equation for the vibrations of a rectangular plate [20]:

$$\mathbf{u}(\mathbf{r}) = \sum_{\eta,\mathbf{q}_\parallel} \sqrt{\frac{\hbar}{2\rho A\omega_\eta}}[a_\eta(\mathbf{q}_\parallel) + a_\eta^+(-\mathbf{q}_\parallel)] \times \mathbf{w}_\eta(\mathbf{q}_\parallel, z)\exp(i\mathbf{q}_\parallel\mathbf{r}_\parallel). \quad (2)$$

Here $a_\eta^+(\mathbf{q}_\parallel)$ and $a_\eta(\mathbf{q}_\parallel)$ are phonon creation and annihilation operators and ω_η is the set of normal vibration frequencies corresponding to the branches (ξ) of the three types (α) of eigenmodes $\eta = (\alpha = \{h,d,f\},\xi = 1,2,\ldots)$, where h is horizontal shear, d is the dilatational mode, and f is the flexural mode. The quantum amplitudes $\mathbf{w}_\eta(\mathbf{q}_\parallel, z)$ are orthonormalized over the thickness L:

$$\int_{-L/2}^{L/2} \mathbf{w}_\eta(\mathbf{q}_\parallel, z)^\dagger \mathbf{w}_{\eta'}(\mathbf{q}_\parallel, z)dz = \delta_{\eta,\eta'}. \quad (3)$$

The deformation potential coupling (see, e.g., [4]) $H_{e\text{-}p} = \frac{2}{3}E_F\int_{V_e} d^3\mathbf{r}\ \Psi^\dagger(\mathbf{r})\Psi(\mathbf{r})\nabla\cdot\mathbf{u}(\mathbf{r})$ (where $E_F = \hbar^2k_F^2/2m$ is the Fermi energy; see also the discussion for Cu in [15]) is then determined by the divergence of the displacement vector and takes the following form in the second quantization:

$$H_{e\text{-}p} = \sum_{\mathbf{k}_\parallel,\mathbf{q}_\parallel,\eta,k_z,k_z'} \left[g_{\eta,\mathbf{q}_\parallel}^{k_z,k_z'} c^\dagger_{\mathbf{k}_\parallel+\mathbf{q}_\parallel,k_z'} c_{\mathbf{k}_\parallel,k_z}\, a_\eta(\mathbf{q}_\parallel) + \left(g_{\eta,\mathbf{q}_\parallel}^{k_z,k_z'}\right)^* c^\dagger_{\mathbf{k}_\parallel-\mathbf{q}_\parallel,k_z'}\, c_{\mathbf{k}_\parallel,k_z} a_\eta^\dagger(\mathbf{q}_\parallel)\right]. \quad (4)$$

Here $c^+_{\mathbf{k}_\parallel,k_z}$ and $c_{\mathbf{k}_\parallel,k_z}$ are the electron creation and annihilation operators; the electron-phonon matrix elements are given by the expression

$$g_{\eta,\mathbf{q}_\parallel}^{k_z,k_z'} = \frac{2}{3}E_F\sqrt{\frac{\hbar}{2\rho A\omega_\eta}}\int_{L/2-d}^{L/2} \psi^*(k_z';z) \times \psi(k_z;z)\left(i\mathbf{q}_\parallel\cdot\mathbf{w}_\eta(\mathbf{q}_\parallel,z) + \frac{\partial w_\eta^z(\mathbf{q}_\parallel,z)}{\partial z}\right)dz. \quad (5)$$

Note that for the considered quasi-two-dimensional geometry the momentum conservation rule works only for the in-plane components of the wave vectors, $\mathbf{k}_\parallel' = \mathbf{k}_\parallel \pm \mathbf{q}_\parallel$, and the electron-phonon coupling allows scattering with the change of the k_z component. The coordinate system is oriented in the plane as shown in Fig. 1 so that we choose x to correspond to the propagation direction of the wave $\mathbf{q}_\parallel = (q,0,0)$. Then from the displacement patterns of the three eigenmodes, $\mathbf{w}_h(q,z) = (0,w_h^y,0)$ and $\mathbf{w}_{d,f}(q,z) = (w_{d,f}^x,0,w_{d,f}^z)$, one can easily see that only the d and f modes couple to electrons. The amplitudes resulting from the solutions of the elasticity equations for the free surface boundary conditions can be represented as follows (the mode index is omitted whenever this does not cause confusion) (see [33,34]):

$$w_d^x = iq_tF_d\left[2q^2\cos\left(\frac{q_tL}{2}\right)\cos(q_lz) + \left(q_t^2-q^2\right)\cos\left(\frac{q_lL}{2}\right)\cos(zq_t)\right],$$

$$w_d^z = qF_d\left[-2q_tq_l\cos\left(\frac{q_tL}{2}\right)\sin(q_lz) + \left(q_t^2-q^2\right)\cos\left(\frac{q_lL}{2}\right)\sin(zq_t)\right] \quad (6)$$

and

$$w_f^x = iq_tF_f\left[2q^2\sin\left(\frac{q_tL}{2}\right)\sin(q_lz) + \left(q_t^2-q^2\right)\sin\left(\frac{q_lL}{2}\right)\sin(zq_t)\right],$$

$$w_f^z = qF_f\left[2q_tq_l\sin\left(\frac{q_tL}{2}\right)\cos(q_lz) - \left(q_t^2-q^2\right)\sin\left(\frac{q_lL}{2}\right)\cos(zq_t)\right]. \quad (7)$$

The multipliers F_d and F_f are determined by the normalization condition (3). The above expressions are equivalent to Eqs. (10), (11), (15), and (16) obtained in [20], as can be easily checked by taking into account that the auxiliary parameters (q_t,q_l) satisfy the eigenfrequency equations:

$$\frac{-4q^2q_lq_t}{(q^2-q_t^2)^2} = \frac{\tan(q_tL/2)}{\tan(q_lL/2)}, \quad (8)$$

for the dilatational mode, and

$$\frac{-4q^2q_lq_t}{(q^2-q_t^2)^2} = \frac{\tan(q_lL/2)}{\tan(q_tL/2)}, \quad (9)$$

for the flexural mode. The closure equation is secured by the "Snell law":

$$\omega = c_l\sqrt{q_l^2+q^2} = c_t\sqrt{q_t^2+q^2}, \quad (10)$$

where $c_{l,t}$ are the longitudinal and transverse sound velocities of the material with the Lame coefficients λ and μ and mass density ρ:

$$c_t = \frac{\mu}{\rho};\quad c_l = \frac{\lambda+2\mu}{\rho}:\ J \equiv c_t^2/c_l^2 < 1/2.$$

From the analysis of the solutions [20,34], it follows that to obtain an explicit expression for the leading low-temperature terms of P it is sufficient to consider the lowest-energy part of the phonon spectra (i.e., acoustical waves), so that the branch index $\xi = 1$ can now be dropped, $\omega_\eta(q) = \omega_{\alpha=d,f}$. Then auxiliary parameters for the f mode are both purely imaginary ($q_{t.l} = ip_{t,l}$), while for the d wave q_t is real and $q_l = ip_l$ is imaginary. After lengthy but straightforward calculations we obtain the explicit form of the solution of the above equations in the long-wavelength approximation:

$$\omega_d \simeq 2qc_t\sqrt{1-J},\quad F_d^{-2} \simeq 16q^6(3-4J)(1-J)^2L,$$
$$q_t^d \simeq q\sqrt{3-4J},\quad p_l^d \simeq q(1-2J), \quad (11)$$

$$\omega_f \simeq q^2Lc_t\sqrt{(1-J)/3},\quad F_f^{-2} \simeq (q^2L)^6L(1-J)^2/36,$$
$$p_t^f \simeq -q+q^3L^2(1-J)/6,\quad p_l^f \simeq -q+q^3L^2J(1-J)/6. \quad (12)$$

These expressions can now be used for the calculation of the electron-phonon matrix elements (5):

$$\left|g_{\alpha,\mathbf{q}_\parallel}^{k_z,k_z'}\right|^2 = |F_\alpha|^2\left[q_t q\left(q_l^2+q^2\right)\right]^2 \frac{8\hbar E_F^2}{9\rho A\omega_\alpha} \times \begin{Bmatrix}\cos^2(Lq_t/2),\alpha=d\\ \sin^2(Lq_t/2),\alpha=f\end{Bmatrix} S(k_z,k_z',\alpha,q_l), \quad (13)$$

where the overlap integral $S(k_z,k_z',\alpha,q_l=ip_l)$ is

$$S(k_z,k_z',\alpha,q_l=ip_l) = \left|\int_{L/2-d}^{L/2}\psi^*(k_z';z)\psi(k_z;z)\begin{Bmatrix}\cosh(zp_l),\alpha=d\\ \sinh(zp_l),\alpha=f\end{Bmatrix}dz\right|^2. \quad (14)$$

As we have already mentioned, the scattering processes described by the Hamiltonian (4) do not require conservation of the z component of the electron wave vector. However, in the long wave limit the overlap integrals can be approximated by taking $\cosh(zp_l)\simeq 1$ and $\sinh(zp_l)\simeq zp_l$ in (14) and using the orthonormality of the $\psi(k_z;z)$. The respective expressions for the d and f modes simplify to

$$S(k_z,k_z',d,q_l=ip_l)=\delta_{k_z,k_z'}, \quad (15)$$

and

$$S(k_z,k_z',f,q_l=ip_l)=|p_l|^2\left|\int_{L/2-d}^{L/2}z\psi^*(k_z';z)\psi(k_z;z)dz\right|^2. \quad (16)$$

Thus, in the long-wavelength approximation the interaction with dilatational modes effectively preserves the electron momentum k_z, unlike the interaction with flexural modes. As discussed in the Introduction, we assume the plane-wave expression for the $\psi(k_z;z)$ function:

$$\psi(k_z;z)=\sqrt{\frac{1}{d}}\exp[ik_z(z+d-L/2)]. \quad (17)$$

This implies, as pointed out in [23] for the case of a nanowire, that the electron-phonon coupling containing integrals like that in Eq. (16) diverges with the thickness of the film. However, below it will be seen that this divergence is removed by the proper normalization of the phonon eigenmodes [F_d and F_f in Eqs. (11) and (12)] in the volume of the sample V_p and the electron-phonon matrix element (13) remains finite.

III. HEAT FLUX CARRIED BY LAMB MODES

We can now calculate the power function P, i.e., the energy transferred from hot electrons to phonons in a unit of time:

$$P=2\sum_{\mathbf{k}_\parallel,\mathbf{q}_\parallel,\alpha,k_z,k_z'}\hbar\omega_\alpha\left[\Gamma^{\rm em}_{\alpha,k_z,k_z'}(\mathbf{k}_\parallel\to\mathbf{k}_\parallel-\mathbf{q}_\parallel) - \Gamma^{\rm ab}_{\alpha,k_z,k_z'}(\mathbf{k}_\parallel\to\mathbf{k}_\parallel+\mathbf{q}_\parallel)\right]. \quad (18)$$

The emission and absorption rates Γ are given by the golden rule:

$$\Gamma^{\rm em}(\mathbf{k}_\parallel\to\mathbf{k}_\parallel-\mathbf{q}_\parallel) = \frac{2\pi}{\hbar}\left|g_{\alpha,\mathbf{q}_\parallel}^{k_z,k_z'}\right|^2[n_p(\hbar\omega_\alpha)+1]f(\epsilon_{\mathbf{k}_\parallel,k_z}) \times[1-f(\epsilon_{\mathbf{k}_\parallel-\mathbf{q}_\parallel,k_z'})]\,\delta\left(\epsilon_{\mathbf{k}_\parallel,k_z}-\epsilon_{\mathbf{k}_\parallel-\mathbf{q}_\parallel,k_z'}-\hbar\omega_\alpha\right), \quad (19)$$

where electron (e) and phonon (p) indices identify the respective temperature in the Bose distribution function $n_{p,e}(\hbar\omega_\alpha)=\{\exp(\beta_{p,e}\hbar\omega_\alpha)-1\}^{-1}$ with $\beta_{p,e}=1/k_BT_{p,e}$; in the Fermi distribution function the chemical potential is replaced by the Fermi energy for the considered low-temperature regime $f(\epsilon_{\mathbf{k}})=\{\exp[\beta_e(\epsilon_{\mathbf{k}}-E_F)]+1\}^{-1}$. The phonon absorption part of Eq. (18), $-\Gamma^{\rm ab}_\alpha(\mathbf{k}\to\mathbf{k}+\mathbf{q}_\parallel)$, is obtained from the emission term $\Gamma^{\rm em}_\alpha(\mathbf{k}\to\mathbf{k}-\mathbf{q}_\parallel)$ by the space-time inversion ($\mathbf{q}_\parallel\to-\mathbf{q}_\parallel$ and $\omega_\alpha\to-\omega_\alpha$) using the identity for the Bose distribution $n(-y)+1=-n(y)$. The power function $P(T)$ can then be cast in the form of a difference between terms separately dependent on T_e and T_p, as in Eq. (1), with the help of the following identity for the Fermi and Bose distribution functions:

$$f(x)[1-f(x-y)]=n_e(y)[f(x-y)-f(x)]. \quad (20)$$

Summation over momenta in Eq. (18) is replaced by integration in a standard way. In calculating the integrals one can then switch to electron density of states and carry out energy integration by using the identity

$$\int_0^\infty[f(x-y)-f(x)]dx = k_BT_e\ln\left(\frac{\exp(\beta_e y)+\exp(-\beta_e E_F)}{1+\exp(-\beta_e E_F)}\right), \quad (21)$$

where the variable y is defined by the phonon energy $y=\pm\hbar\omega_\alpha$ in the emission and absorption processes [see Eqs. (18)]. Taking into account that $\hbar\omega_\alpha,k_BT\ll E_F$, the exponentially small terms in the round brackets on the right-hand side of Eq. (21) can be neglected and we obtain the relation

$$\int_0^\infty[f(x-y)-f(x)]dx\simeq y, \quad (22)$$

also used in [21]. However, a more physically transparent way is to note that at low temperatures the electron scattering takes place near the Fermi surface, i.e., $\hbar\omega_\alpha,k_BT\ll\epsilon_{\mathbf{k}}\sim E_F$. This allows us to approximate the right-hand side of Eq. (20) with $n_e(y)y\delta(\epsilon_{\mathbf{k}}-E_F)$, by using the known expression for the main term of the expansion $f(x-y)-f(x)\simeq-y\partial f/\partial x\simeq y\delta(\epsilon_{\mathbf{k}}-E_F)$ [see, e.g., Eq. (5.42) in [35]]. It can also be seen that this approximation reproduces the result in Eq. (22); recall that $x=\epsilon_k$. Then the above-mentioned form of Eq. (18) is easily obtained as follows:

$$P=P_0(T_e)-P_0(T_p). \quad (23)$$

Here

$$P_0(T_e)=\sum_{\mathbf{k}_\parallel,k_z,k_z',\mathbf{q}_\parallel,\alpha=d,f}\frac{32\pi\hbar^2E_F^2}{9\rho A}\omega_\alpha|F_\alpha|^2\left[q_tq\left(q_l^2+q^2\right)\right]^2 \times n(\hbar\omega_\alpha/k_BT_e)\delta(\epsilon_{\mathbf{k}}-E_F)\begin{Bmatrix}\cos^2(Lq_t/2),\alpha=d\\ \sin^2(Lq_t/2),\alpha=f\end{Bmatrix} \times S(k_z,k_z',\alpha,q_l)\delta(\epsilon_{\mathbf{k}_\parallel,k_z}-\epsilon_{\mathbf{k}_\parallel-\mathbf{q}_\parallel,k_z'}-\hbar\omega_\alpha). \quad (24)$$

Equation (24) shows that in this leading order of the low-temperature expansion the initial state of electrons is on the Fermi surface, while the change of electron energy in the scattering process is of the order of k_BT (the average phonon energy).

Let us now consider the energy conservation condition imposed by the last δ function in Eq. (24) on the cosine of the angle between the electron and phonon wave vectors written in spherical coordinates ($\sin\theta\cos\varphi$):

$$\delta\left\{\frac{\hbar^2}{m}(k_F q\sin\theta\cos\varphi)+\frac{\hbar^2}{2m}\left[k_z^2-(k_z')^2-q^2\right]-\hbar\omega_\alpha\right\}. \tag{25}$$

For the dilatational mode ($\alpha = d$) we have $k_z' = k_z$ from Eq. (15) and then from Eq. (24) we obtain

$$P_0^{FG,d}(T_e)=\frac{32\pi\hbar^2E_F^2}{9\rho A}\frac{Ad}{(2\pi)^3}\int_0^\infty k^2dk\int_0^\pi\sin\theta d\theta\int_0^{2\pi}d\phi\frac{A}{(2\pi)^2}\left(\int_0^\infty\int_0^{2\pi}qdqd\phi_d\right)$$
$$\times\,\omega_d|F_d|^2\left[q_tq(q_l^2+q^2)\right]^2n_e(\hbar\omega_d)\delta\left(\frac{\hbar^2k^2}{2m}-E_F\right)\cos^2(Lq_t/2)\frac{m}{\hbar^2kq}\delta\left(\sin\theta\cos\phi-\frac{q}{2k}-\frac{m\omega_d(q)}{\hbar kq}\right). \tag{26}$$

One can see that due to conservation of the z component of the electron momentum the phonon is actually emitted in the direction orthogonal to $\mathbf{k}$, i.e., $|\sin\theta\cos\varphi|\ll 1$. Indeed, we can estimate $m\omega_d/\hbar k_F q\sim c_t/v_F\ll 1$ and, since $k_F\sim\pi/a_0$ (a_0 is the lattice spacing), also $q/2k_F\ll 1$. So, the $\mathbf{k}$ vector is allowed to rotate without restrictions in the plane orthogonal to $\mathbf{q}_\parallel$, while $\mathbf{q}_\parallel$ in its turn is free to rotate in the plane of the film. Thus, integration over the electron (θ,ϕ) and phonon (ϕ_d) angles in Eq. (26) results in the multiplier $(2\pi)^2$ (formal derivation is somewhat lengthier and leads to the same conclusion). Integration over the length of $\mathbf{k}$ is trivial and can also be expressed in terms of the electron density of states for the parabolic dispersion, $N(E_F)=Admk_F/(\hbar\pi)^2$. We finally obtain the following expression for the d mode:

$$P_{0,d}(T_e)=\frac{32\pi m^2E_F^2}{9\rho\hbar^2}\frac{Ad}{(2\pi)^3}\int_0^\infty\omega_d|F_d|^2\left[q_tq\left(q_l^2+q^2\right)\right]^2n_e(\hbar\omega_d)\cos^2(Lq_t/2)dq, \tag{27}$$

which after substitution of the expressions in Eq. (11) into Eq. (27) results in

$$P_{0,d}(T_e)=\frac{\zeta(4)}{12\pi^2}\frac{V_e(k_BT_e)^4k_F^4J^2}{\rho L\hbar^2c_t^3(1-J)^{3/2}}. \tag{28}$$

Calculation of the heat current due to the flexural phonon modes is more involved since k_z is not conserved even in the long-wavelength approximation and can significantly differ from k_z', Eq. (16). It is then convenient to express the power function (24) in the cylindrical coordinates:

$$P_{0,f}(T_e)=\frac{16E_F^2}{9\rho}\frac{Ad^4}{(2\pi)^4}\left(\frac{m}{\hbar}\right)^2\int_0^\infty dqI(q)|p_l|^2\omega_\alpha|F_\alpha|^2\left[q_tq\left(q_l^2+q^2\right)\right]^2n(\hbar\omega_q/k_BT_e)\sin^2(Lq_t/2). \tag{29}$$

Here

$$I(q)=\int_0^{k_F}\frac{dk_\parallel}{\sqrt{k_F^2-k_\parallel^2}}\int_{-k_F}^{k_F}dk_z\int_{-\infty}^{\infty}dk_z'\left[\delta\left(k_z-\sqrt{k_F^2-k_\parallel^2}\right)+\delta\left(k_z+\sqrt{k_F^2-k_\parallel^2}\right)\right]$$
$$\times\left|\int_{\sigma/2-1}^{\sigma/2}\exp(id(k_z-k_z')z)zdz\right|^2\int_0^{2\pi}d\phi\delta\left(\cos\phi+\frac{\left[k_z^2-(k_z')^2-q^2\right]/2}{k_\parallel q}-\frac{m\omega_f}{\hbar k_\parallel q}\right). \tag{30}$$

In Eq. (30) we have introduced the ratio $\sigma = L/d$ with the limit value $\sigma = 1$ corresponding to the absence of the insulating membrane, i.e., to a purely metallic sample. The multiple integral $I(q)$ is calculated analytically in the Appendix and its substitution into Eq. (29), together with the solution (12) for the flexural mode, leads to the following expression:

$$P_{0,f}(T_e)=\frac{V_e(k_BT_e)^4d^3m^2J^2E_F^2}{4\sqrt{3}\pi^3\rho L^4c_t^3\hbar^6(1-J)^{3/2}}\left[(\sigma-1)^2\int_0^\infty x^3(-\ln x)n(x)dx\right.$$
$$\left.+\left[\frac{1}{2}+(\sigma-1)^2\ln\left(25.53\frac{\hbar Lc_t\sqrt{(1-J)/3}}{d^2k_BT_e}\right)\right]\int_0^\infty x^3n(x)dx\right]. \tag{31}$$

From Eq. (31) we obtain the final result for the contribution of the flexural modes:

$$P_{0,f}(T_e)=\frac{0.0075V_e(k_BT_e)^4k_F^4J^2}{\rho L\sigma^3\hbar^2c_t^3(1-J)^{3/2}}\left((\sigma-1)^2\ln\left[4.4\frac{\sigma^2\hbar c_t\sqrt{1-J}}{Lk_BT_e}\right]+\frac{1}{2}\right). \tag{32}$$

The argument in the square brackets is proportional to $T^*/T_e\sim\hbar c/(Lk_BT_e)$, so that the log term is positive for temperature in the interval below the crossover, i.e., where the description of the phonon subsystem in terms of quasi-two-dimensional phonon confinement is applicable. Note also that $P_{0,f}(T_e)$ does not vanish even for a purely metallic slab

($V_e = V_p$ and $\sigma = 1$) when electrons experience an antisymmetric field created by the flexural vibration mode [Eq. (16)] and the respective overlap function vanishes $S(k_z = k_z', f, q_l = ip_l) = 0$. This result demonstrates the point made in the Introduction that the nonzero contribution of the flexural modes to the heat transfer is due to scattering processes with $k_z' \neq k_z$. One can also see that the above result scales with the surface of the sample ($P \sim A$) for a free metallic film ($\sigma = 1$), but for a composite structure ($\sigma > 1$) the geometry dependence becomes more complicated even for an acoustically uniform medium.

To simplify the discussion we assume that the phonon temperature is much lower than T_e, so that the total density of the heat transfer power Q is obtained as the sum of just the two contributions in Eqs. (28) and (32):

$$Q = (P_{0,d}(T_e) + P_{0,f}(T_e))/V_e. \tag{33}$$

Thus, for the considered case of an acoustically uniform metal-insulator composite slab we obtain the following expression:

$$Q = \frac{0.0075(k_B T_e)^4 k_F^4 J^2}{\rho L \sigma^3 \hbar^2 c_t^3 (1-J)^{3/2}} \left[1.2\sigma^3 + \frac{1}{2} + (\sigma - 1)^2 \times \ln\left(4.4 \frac{\hbar \sigma^2 c_t \sqrt{1-J}}{L k_B T_e} \right) \right]. \tag{34}$$

Its generalization to the case of two acoustically inequivalent rigidly bonded layers is much lengthier and will be presented in detail elsewhere. A typical example corresponds to a Cu film deposited on a silicon-nitride insulating membrane. Following the guidelines of the standard description of layered elastic media (see, e.g., [25,26]), one can obtain the analytic solutions for the acoustic branches of the vibrational modes and respective normalization factors in the long-wavelength approximation. The result is that solutions of the Stoneley type (i.e., interface guided waves with the amplitude decreasing away from the interface) do not appear in the long-wavelength limit and it is well justified to keep the two types of modes considered above solely responsible for the low-temperature behavior also in this case.

We identify the material parameters corresponding to Cu and silicon nitride by the respective indices, $i = 1$ and 2. The mass of the composite slab is M and the ratio M/A replaces the product ρL in Eq. (34). Then, with the additional notations

$$R_i = \rho_i c_{t,i}^2 (1 - J_i), \quad \chi = \frac{1}{2}\left(\frac{R_2(L-d)^2 - R_1 d^2}{R_2(L-d) + R_1 d} \right),$$
$$G = \frac{2\hbar}{d^2} \sqrt{\frac{[R_1 d^3 + R_2(L-d)^3]/3 - \chi^2 [R_1 d + R_2(L-d)]}{\rho_1 d + \rho_2 (L-d)}}, \tag{35}$$

the long-wavelength dispersion of the dilatational acoustic mode can be written as

$$\omega_d = 2q \sqrt{\frac{R_1 d + R_2(L-d)}{\rho_1 d + \rho_2 (L-d)}}. \tag{36}$$

Equation (36) reproduces the known result [32]. For the flexural mode we find

$$\omega_f = 2q^2 \sqrt{\frac{[R_1 d^3 + R_2(L-d)^3]/3 - \chi^2 [R_2(L-d) + R_1 d]}{\rho_1 d + \rho_2 (L-d)}}. \tag{37}$$

It is easy to check that these expressions correctly reproduce the limit of the acoustically uniform medium and amount to an effective renormalization of the parameters in Eq. (34) without qualitatively changing the temperature dependence. Indeed, by carrying out the calculations within the lines described in the previous case we obtain the following generalization of Eqs. (31)–(33) for the power density function $Q(T_e) = Q_d(T_e) + Q_f(T_e)$, where

$$Q_d = (k_B T_e)^4 \frac{\zeta(4)}{12\pi^2} \frac{A k_F^4 J_1^2}{\hbar^2 M} \left(\frac{\rho_1 d + \rho_2 (L-d)}{R_1 d + R_2 (L-d)} \right)^{3/2}, \tag{38}$$

$$Q_f = \frac{(\kappa_B T_e)^4}{\pi^3 3^2 2^7} \frac{A k_F^4 J_1^2}{\hbar^2 M} \{(2\chi/d + 1)^2 [\ln(G/k_B T_e) + 13.3] + 3.247\} \left(\frac{d^2 [\rho_1 d + \rho_2 (L-d)]}{[R_1 d^3 + R_2 (L-d)^3]/3 - \chi^2 [R_2 (L-d) + R_1 d]} \right)^{3/2}. \tag{39}$$

Figure 2 shows the relative contribution of the two modes as given by Eqs. (38) and (39) to the electron-phonon heat transfer (Q_f/Q_d) for the two samples $M1$ and $M3$ which have been interpreted in [12,13] as demonstrating a crossover in the sub-Kelvin region. The material parameters can be found in [12,13,15]: $\rho_1 = 8940$ kg/m^3, $\rho_2 = 3290$ kg/m^3, $c_{t,1} = 2575$ m/s, $c_{t,2} = 6200$ m/s, $J_1 = 0.27$, $J_2 = 0.36$, $L = 30$ nm, $A = 600 \times 300 (\mu\text{m})^2$, $d(M1) = 14$ nm, $d(M3) = 19$ nm, to a good approximation $M/A \simeq \rho_2 (L-d)$ by taking into account that the surface of the Cu film in these experiments was smaller than the supporting membrane. The value of $k_F = 1.65 \times 10^{10}$ m^{-1} in the prefactor of the above equations is discussed below.

We can see that the contribution of the flexural mode to the heat transfer is comparable to the dilatational one and gains more "weight" towards lower temperatures due to the presence of the log term in Eq. (39). Moreover, Fig. 2 indicates that the sample with a higher thickness ratio between the metal film and the insulating membrane (i.e., a smaller geometric factor: $\sigma(M3) = 49/19 < \sigma(M1) = 44/14$ has also a higher value of the power ratio Q_f/Q_d. Note also that the ratio Q_f/Q_d reduces to a constant ($\simeq 0.41$) for the case of a suspended

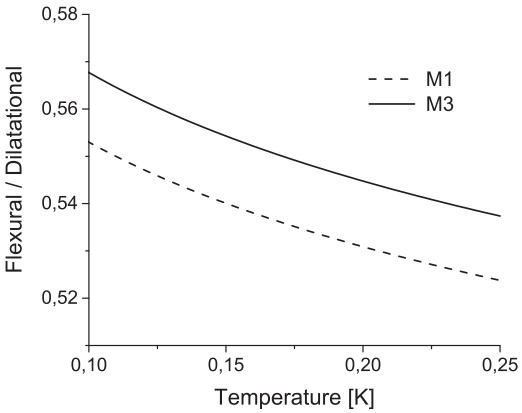

FIG. 2. The relative contribution Q_f/Q_d, Eqs. (38) and (39), to the heat flux of the flexural vs dilatational acoustic modes for the two samples $M1$ and $M3$ in [12,13] (see text).

metallic film, as can be easily seen from Eqs. (28) and (32) with $\sigma = 1$.

In Fig. 3 our result is compared to the temperature dependence of the total power density $Q = Q_f + Q_d$ for the sample $M1$ (Fig. 3 in [12]) with the material parameters as given above. The effective value of k_F is obtained by fitting the low-temperature region of $Q(T)$ and is slightly larger than 1.4×10^{10} m^{-1} following from the known value of the Fermi energy for copper, 7 eV, if the effective mass m is estimated from the electron heat capacity (e.g., [36]) for the simple isotropic parabolic dispersion. We mention that in [15] the deviation of the Fermi surface in noble metals from a simple spherical shape has been studied in terms of surface averaged effective electronic parameters and for Cu the estimated increase of the respective prefactor in the electron-phonon power function is comparable to our result.

At temperatures above 250 mK the analytical curve starts to deviate from the experiment as the crossover temperature is approached and higher-energy branches of the Lamb modes spectrum should be taken into account. From Eqs. (38) and (39) it also follows that the $M3$ sample (not shown in Fig. 3) has a somewhat higher value of the total power density Q than $M1$ for the considered temperature region. The quantitative comparison shows a good agreement with the results presented in Fig. 4 of [12] and in Fig. 3 of [13].

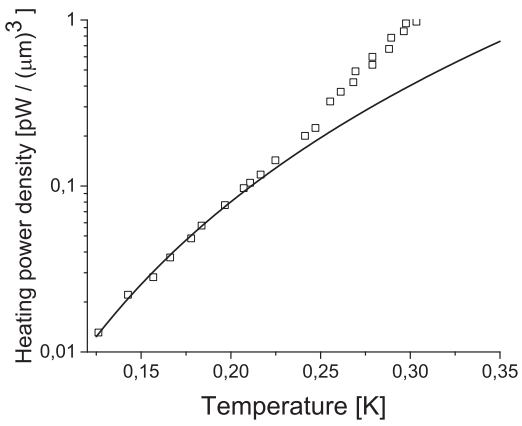

FIG. 3. The power density of the electron-phonon heat transfer for the $M1$ sample in [12] (squares) and the joint contribution due to flexural and dilatational acoustical Lamb modes $Q = Q_f + Q_d$ as given by Eqs. (38) and (39) (see text).

IV. CONCLUSIONS

We have obtained explicit expressions for the power density of the electron-phonon heat transfer in a metallic film including the case when the film is deposited on an insulating membrane with generally different acoustic characteristics, Eqs. (38) and (39). The temperature regime covered by the present analysis corresponds to low temperatures when the phonon spectrum is dominated by quasi-two-dimensional modes of vibration. The long-wavelength approximation which considers only the lowest phonon branches is well justified at lower temperatures and has allowed us to carry out the calculations analytically. Thus, for the specific example considered above, e.g., Fig. 3, this description corresponds to temperatures below 0.25 K while the quasi-two-dimensional regime sets in around 0.4–0.5 K [12]. It turns out that the contributions of the flexural and dilatational phonon modes to the heat flux are of the same order of magnitude, as illustrated by Fig. 2.

For a suspended metallic film, $\sigma = 1$, the heat current follows a T^4 dependence, i.e., $P = \Sigma_{2D} A(T_e^4 - T_p^4)$, which appears to fit the pattern of the dimensionality dependence including the integer power x in the T^x temperature variation, namely, when the phonon subsystem corresponds to either a three-dimensional bulk material with the power index $x = 5$ as in Eq. (1), or to a two-dimensional or quasi-two-dimensional material such as a single or bilayer graphene [37,38] with $x = 4$, or to a quasi-one-dimensional nanowire [17] with $x = 3$. However, this result could seem surprising in the context of previous works on some other quasi-two-dimensional systems, e.g., [20,21], for the case of a semiconductor quantum well, which would rather suggest a fractional value of x due to the peculiar quadratic dispersion of the flexural mode. Fractional power, $T^{2.5} \ln T$, was also reported for the flexural modes' contribution to electrical resistivity in free-standing graphene [39]. The value $x = 4$ for the heat flux in graphene is actually due to electron coupling with the dilatational phonons, since the "troublesome" flexural ones couple to electrons only in second order in the displacement and can be disregarded for the graphene on a substrate as well [37]. Moreover, essentially different contributions of the phonon modes could be expected to result not only from the linearity and nonlinearity of the respective dispersion laws but also from the explicit presence of the size (thickness L) dependence in the dispersion of the flexural mode [e.g., compare ω_d and ω_f in Eqs. (11) and (12)]. Indeed, in the studies on phonon transport and phonon heat capacity of a free-standing dielectric membrane [40,41] a striking difference between the thickness dependent and nondependent behavior has been derived for the two types of vibration. In contrast, for the electron-phonon heat transfer we find a comparable contribution for the two modes even when the metallic film is deposited on an insulating membrane ($\sigma > 1$), when the effect of sample geometry on the power P is more complicated than a simple scaling with surface area A [see, e.g., Eqs. (28) and (32) for the acoustically uniform sample]. As we have shown such unexpected relative similarity

in the temperature and size (e.g., thickness) dependence results from several physical factors, so that their combination differs from the cases studied earlier. For a coupled electron-phonon system both the dispersions and the amplitudes of the excitations play an important role. Respectively, a proper normalization of the amplitudes is crucial. One can then see, e.g., from Eqs. (11) and (12), that the normalization of the phonon modes in Eqs. (6) and (7) containing the multipliers $F_{d,f}$ and the auxiliary parameters $q_{t,l}$, moderates to some extent the sharp differences between the d and f dispersions. It is also clear that this "compensation" depends on specific quantity considered, which in our case is the heat flux. Unlike the case of graphene or that of a semiconductor quantum well, the electron excitations are described in terms of three-dimensional Fermi gas with parabolic dispersion. Respectively, the overlap of the electronic amplitudes in the initial and scattered states [Eq. (14)] is also a physical factor which differs from the models considered before. As discussed in the text, this overlap strongly discriminates between the d and f phonons and contributes to the above-mentioned "compensation" as well.

For the case of a metallic film deposited on an insulating membrane the flexural mode contribution to the power density of the electron-phonon heat transfer acquires an additional logarithmic term of the form $T^4 \ln T$ [Eq. (39)], while that of dilatational modes keeps the T^4 dependence [Eq. (38)]. As we have shown, such functional dependence reproduces well the observed behavior, which was modeled in [12] with a power law T^x with $x < 4.5$. The dependence on the material parameters for a metallic film with dielectric backing becomes more complicated, especially for the acoustically nonuniform case. This point can be illustrated by a more detailed analysis of the experimental work cited above. Thus, one generally expects that reducing the dimensionality would enhance the electron-phonon heat exchange. This is confirmed by Figs. 2 and 4 in [12] for sufficiently thick samples to be considered bulklike (e.g., $M5$ and $B1$) and which show a much lower power density Q ($=P/V_e$) than the thinner samples (like $M1$ and $M3$ discussed earlier, with $M3$ being thicker than $M1$). Moreover, if the simple surface area scaling of the power function ($P \sim A$) would be valid for these thinner samples, then one would expect that $Q(M1) > Q(M3)$. However, the power density for the thicker of the two ($M3$) is larger than for the thinner one ($M1$) in the considered temperature region. This nontrivial dependence on the material parameters is well reproduced by the analytical expressions. Thus, the present analysis demonstrates that in thin metal films both types of Lamb's phonon modes should be taken into account on equal footing for a better understanding of the electron-phonon heat transfer at low temperatures.

ACKNOWLEDGMENT

This work has been financially supported by UEFISCDI (Romania), Project No. Idei-PCE 114/2011, and by ANCS, Project No. PN09370102.

APPENDIX

Integration over the angle ϕ and over k_z in Eq. (30) reduces to a triple integral:

$$I(q) = \int_0^{k_F} \frac{dk_\parallel}{\sqrt{k_F^2 - k_\parallel^2}} \int_{-\infty}^{\infty} dk_z' \frac{\theta\left(1 - \left\{\left[k_F^2 - k_\parallel^2 - (k_z')^2\right]/2k_\parallel q - Dq/k_\parallel\right\}^2\right)}{\sqrt{1 - \left\{\left[k_F^2 - k_\parallel^2 - (k_z')^2\right]/2k_\parallel q - Dq/k_\parallel\right\}^2}}$$
$$\times \left(\left| \int_{\sigma/2-1}^{\sigma/2} \exp\left(id\left(\sqrt{k_F^2 - k_\parallel^2} - k_z'\right)z\right) z dz \right|^2 + \left| \int_{\sigma/2-1}^{\sigma/2} \exp\left(id\left(\sqrt{k_F^2 - k_\parallel^2} + k_z'\right)z\right) z dz \right|^2 \right), \tag{A1}$$

where $\theta(x)$ is the Heaviside function and we have introduced the constant

$$D = 1/2 + mLc_t\sqrt{(1-J)/3}/\hbar > 0,$$

taking into account the dispersion of the flexural mode in Eq. (12).

We further use the dimensionless variables

$$x = \sqrt{k_F^2 - k_\parallel^2}/k_F, \quad y = k_z'/k_F, \quad Q = q/k_F. \tag{A2}$$

Equation (A1) then transforms into

$$I(q) = 2q \int_0^1 dx \int_{-\infty}^{\infty} dy \frac{\theta[4Q^2(1-x^2) - (x^2 - y^2 - 2DQ^2)^2]}{\sqrt{4Q^2(1-x^2) - (x^2 - y^2 - 2DQ^2)^2}} (G^- + G^+), \tag{A3}$$

where we have defined the functions

$$G^{\mp} \equiv G(y \mp x) = \left| \int_{\sigma/2-1}^{\sigma/2} \exp\left(idk_F(y \mp x)z\right) z dz \right|^2. \tag{A4}$$

We next consider the contribution $I^-(q)$ to $I(q)$ corresponding to G^- and switch to new variables:

$$u = y - x, \quad v = x. \tag{A5}$$

Then $I^-(q)$ takes the following form:

$$I^- = 2q \int_{-\infty}^{\infty} du \left| \int_{\sigma/2-1}^{\sigma/2} \exp(i dk_F u z) z dz \right|^2 \int_0^1 \frac{\theta(c - bv - av^2) dv}{\sqrt{c - bv - av^2}}, \tag{A6}$$

where a,b, and c are functions of u:

$$\begin{aligned} a &= 4(Q^2 + u^2) > 0, \\ b &= 4u(u^2 + 2DQ^2), \\ c &= 4Q^2 - (u^2 + 2DQ^2)^2. \end{aligned} \tag{A7}$$

Integration over v gives

$$\int_0^1 \frac{\theta(c - bv - av^2) dv}{\sqrt{c - bv - av^2}} = \frac{1}{\sqrt{a}} \left[\frac{\pi}{2} - \arctan\left(\frac{b\theta(c)}{2\sqrt{ac}} \right) \right]. \tag{A8}$$

Returning then to the definitions in Eq. (A4) and considering G^+ we now define the variables u and v by changing the sign, respectively: $u = y + x$ and $v = x$. This results in the expression for the $I^+(q)$ which differs from $I^-(q)$ in Eq. (A6) by the change of sign in front of b, so that integration over v will differ from Eq. (A8) by the sign in front of the arctan function. These terms then cancel each other in Eq. (A3) when expressed in the u and v variables, so that our integral simplifies to

$$I = \pi q \int_{-\infty}^{\infty} \left| \int_{\sigma/2-1}^{\sigma/2} \exp(i dk_F u z) z dz \right|^2 \frac{du}{\sqrt{Q^2 + u^2}}. \tag{A9}$$

The z integral can also be integrated exactly, so that after the replacement of variable $x = u dk_F$ Eq. (A9) becomes

$$I = \int_{-\infty}^{\infty} \frac{2\sigma(\sigma - 2)x^2(1 - \cos x) + 4x^2 + 8(1 - \cos x - x \sin x)}{4x^4 \sqrt{(dq)^2 + x^2}} dx. \tag{A10}$$

The last integral can be reduced to the Meijer G function [42], however for the long-wavelength approximation $dq < 1$ one can also obtain directly from Eq. (A10) its excellent approximation for $dq < 1$ by the following expression:

$$I(q) \simeq \pi q \left(-\frac{(\sigma - 1)^2}{2} \ln(dq) + 0.81(\sigma - 1)^2 + \frac{1}{8} \right). \tag{A11}$$

[1] H. Q. Nguyen, M. Meschke, H. Courtois, and J. P. Pekola, Phys. Rev. Appl. **2**, 054001 (2014).

[2] J. T. Muhonen, M. Meschke, and J. P. Pekola, Rep. Prog. Phys. **75**, 046501 (2012).

[3] A. V. Feshchenko, L. Casparis, I. M. Khaymovich, D. Maradan, O.-P. Saira, M. Palma, M. Meschke, J. P. Pekola, and D. M. Zumbuhl, Phys. Rev. Appl. **4**, 034001 (2015).

[4] J. Ziman, *Electrons and Phonons: The Theory of Transport Phenomena in Solids* (Clarendon, Oxford, 1960).

[5] M. I. Kaganov, I. M. Lifshitz, and L. V. Tanatarov, Zh. Eksp. Teor. Fiz. **31**, 232 (1956) [Sov. Phys. JETP **4**, 173 (1957)].

[6] P. B. Allen, Phys. Rev. Lett. **59**, 1460 (1987).

[7] F. C. Wellstood, C. Urbina, and John Clarke, Phys. Rev. B **49**, 5942 (1994).

[8] A. Sergeev and V. Mitin, Phys. Rev. B **61**, 6041 (2000).

[9] J. T. Karvonen, L. J. Taskinen, and I. J. Maasilta, Phys. Rev. B **72**, 012302 (2005).

[10] M. A. Stroscio and M. Dutta, *Phonons in Nanostructures* (Cambridge University Press, Cambridge, England, 2004).

[11] A. N. Cleland, *Foundations of Nanomechanics* (Springer-Verlag, Berlin, 2003).

[12] J. T. Karvonen and I. J. Maasilta, Phys. Rev. Lett. **99**, 145503 (2007).

[13] J. Karvonen and I. Maasilta, J. Phys.: Conf. Ser. **92**, 012043 (2007).

[14] J. F. DiTusa, K. Lin, M. Park, M. S. Isaacson, and J. M. Parpia, Phys. Rev. Lett. **68**, 1156 (1992).

[15] S.-X. Qu, A. N. Cleland, and M. R. Geller, Phys. Rev. B **72**, 224301 (2005).

[16] J. M. Underwood, P. J. Lowell, G. C. O'Neil, and J. N. Ullom, Phys. Rev. Lett. **107**, 255504 (2011).

[17] F. W. J. Hekking, A. O. Niskanen, and J. P. Pekola, Phys. Rev. B **77**, 033401 (2008).

[18] J. T. Muhonen, A. O. Niskanen, M. Meschke, Yu. A. Pashkin, J. S. Tsai, L. Sainiemi, S. Franssila, and J. P. Pekola, Appl. Phys. Lett. **94**, 073101 (2009).

[19] B. A. Auld, *Acoustic Fields and Waves in Solids*, 2nd ed. (Krieger, Malabar, Florida, 1990).

[20] N. Bannov, V. Aristov, V. Mitin, and M. A. Stroscio, Phys. Rev. B **51**, 9930 (1995).

[21] B. A. Glavin, V. I. Pipa, V. V. Mitin, and M. A. Stroscio, Phys. Rev. B **65**, 205315 (2002).

[22] S. K. Mahatha and K. S. R. Menon, J. Electron Spectrosc. **193**, 43 (2014).

[23] Z. Lindenfeld and R. Lifshitz, Phys. Rev. B **87**, 085448 (2013).

[24] P. J. Koppinen and I. J. Maasilta, Phys. Rev. Lett. **102**, 165502 (2009).
[25] L. M. Brekhovskikh, *Waves in Layered Media* (Academic Press, New York, 1980).
[26] J. L. Rose, *Ultrasonic Waves in Solid Media* (Cambridge University Press, Cambridge, England, 2004).
[27] J. D. N. Cheeke, *Fundamentals and Applications of Ultrasonic Waves* (CRC Press, Boca Raton, Florida, 2002).
[28] L. M. A. Pascal, A. Fay, C. B. Winkelmann, and H. Courtois, Phys. Rev. B **88**, 100502(R) (2013).
[29] E. Swartz and R. Pohl, Rev. Mod. Phys. **61**, 605 (1989).
[30] F. Giazotto, T. T. Heikkilä, A. Luukanen, A. Savin, and J. P. Pekola, Rev. Mod. Phys. **78**, 217 (2006).
[31] V. J. Kauppila, H. Q. Nguyen, and T. T. Heikkilä, Phys. Rev. B **88**, 075428 (2013).
[32] Wang Xiao-Min, Lian Guo-Xuan, and Li Ming-Xuan, Chin. Phys. Lett. **20**, 1084 (2003).
[33] D. V. Anghel and T. Kühn, J. Phys. A **40**, 10429 (2007).
[34] T. Kühn, D. V. Anghel, Y. M. Galperin, and M. Manninen, Phys. Rev. B **76**, 165425 (2007).
[35] G. Rickayzen, *Green's Functions and Condensed Matter* (Dover Publication, New York, 2013).
[36] D. L. Martin, Phys. Rev. B **8**, 5357 (1973).
[37] J. K. Viljas and T. T. Heikkilä, Phys. Rev. B **81**, 245404 (2010).
[38] S. S. Kubakaddi, Phys. Rev. B **79**, 075417 (2009).
[39] E. Mariani and F. von Oppen, Phys. Rev. Lett. **100**, 076801 (2008); **100**, 249901(E) (2008).
[40] T. Kühn, D. V. Anghel, J. P. Pekola, M. Manninen, and Y. M. Galperin, Phys. Rev. B **70**, 125425 (2004).
[41] O. V. Fefelov, J. Bergli, and Y. M. Galperin, Phys. Rev. B **75**, 172101 (2007).
[42] *NIST Handbook of Mathematical Functions*, edited by F. W. J. Olver, D. W. Lozier, R. F. Boisvert, and C. W. Clark (Cambridge University Press, Cambridge, England, 2010).